Asociación Argentina
de Mecánica Computacional

Mecánica Computacional Vol XXX, págs. 3-21 (artículo completo)
Oscar Möller, Javier W. Signorelli, Mario A. Storti (Eds.)
Rosario, Argentina, 1-4 Noviembre 2011

COMPUTATIONAL MODELS AND UNCERTAINTIES: ESTIMATION OF RELIABILITY AND RISK

Ricardo O. Foschi

Civil Engineering Department, University of British Columbia, 6250 Applied Sciences Lane, Vancouver, B.C., Canada V6T 1Z4, rowfa1@civil.ubc.ca

Keywords: Uncertainty, Randomness, Reliability, Optimization

Abstract. Great advances in computational mechanics and numerical methods have permitted the solution of complex, previously intractable nonlinear problems either in solid or fluid mechanics. Computers have now sufficient memory and efficient operational systems which allow the solution of problems with a great number of degrees of freedom in a reasonable time. On the other hand, the theoretical models, and their numerical representation, implement relationships between variables which are not necessarily known with precision. These uncertain variables introduce randomness in the results and this, in turn, affects conclusions regarding reliability and quantification of risks. This presentation discusses the need to integrate the deterministic calculations from numerical models with methods to assess the probabilistic nature of the predictions. At the same time, the presentation discusses briefly different strategies to implement the estimation of probabilities, as well as probabilistic design procedures based on the reliable satisfaction of different performance requirements. The discussion is illustrated with two applications: the collision force between an ice mass and an offshore exploration platform, and the collision force between vessels and the piers of a bridge.

1 MODELS, UNCERTAINTIES AND RELIABILITY

Models in computational mechanics normally have, as a base, a corresponding set of differential equations. For example, the foundation for models based on the theory of elasticity incorporate stresses and strains into equations for constitutive material behavior, conditions of equilibrium and compatibility of deformations. These models could represent different levels of complexity, from small deformations leading to linear behavior, to large strains for nonlinear problems. The material representation could also be linear or nonlinear and, in either case, incorporates "material characteristic constants" which have to be determined from experimental testing (e.g., the "modulus of elasticity E"). The incorporation of plastic behavior in the material equations leads to the theory of plasticity and, similarly, the consideration of time effects to the theory of viscoelasticity (either linear or nonlinear). Equilibrium equations could include acceleration and damping terms, needed for the study of dynamic problems. As a general rule, these equations do not admit closed-form solutions except in very simple cases. As a norm, the equations are then solved by numerical means, using either finite difference approximations for derivatives or implementing variational principles resulting in what we know as "finite element methods".

The theoretical models are, of course, approximate interpretations of reality and are subject to some error. The numerical form of the theoretical models incorporate a further error related, for example, to discretization techniques, time step size, convergence criteria, etc. Furthermore, the constants in the material model are not deterministic: the experimental tests required for their evaluation yield different results for each test replication. For example, the modulus of elasticity E would vary from experiment to experiment, and would show spatial variability within a mesh of finite elements. Variability in material properties appear also when considering time effects like creep or relaxation, or when incorporating effects of size. Quantities like density are not uniformly distributed within a given volume and, for example, the density variation in a composite material is dependent on its manufacturing process. Uncertain manufacturing variables like pressing temperature, pressure, rate of cooling after pressing, all influence the final shape of a composite component, a randomness which is of major importance for the use of such composites in aircraft structures. The error in the quantification of the material behavior can be reduced by further testing, and it is said to have an aleatoric base. The model error is intrinsic to our interpretation of reality and it is thus called a source of epistemic uncertainty.

Any application in computational mechanics will then contain a set of intervening random variables. These uncertainties require consideration, using tools of probability theory in conjunction with the computational mechanics model. Two basic problems arise: 1) to determine the probability that an output from the models will exceed a target value, or 2) to calculate the value of a model parameter so that the probability of an output exceeding a threshold in a given performance criterion be as prescribed. The first type of problem falls into the area of reliability evaluation, while the second relates to "*performance-based design*". Since uncertainties, whether epistemic or aleatoric, cannot be avoided, a complete solution of the problem not only requires a robust deterministic computational technique but also a link to a probabilistic assessment of the effect from the uncertainties.

2 PROBLEM FORMULATION AND RELIABILITY ASSESSMENT

In general, the performance of an engineering system can be described by a *performance or limit state function G(x)* , the form of which is

$$G(x) = C(x_c, d_c) - D(x_d, d_d) \ . \qquad (1)$$

G(x) is a function of the intervening random variables and can always be written as the difference between two functions, a *system capacity C* and a *demand D*. The variables may be divided into two groups: one, (x_c , d_c) , related to the capacity *C*, and a second, *(x_d , d_d)* , associated with the demand *D*. The vectors x_c and x_d include all those variables which are random or uncertain, while the vectors d_c and d_d include all those quantities which are either *deterministic* or known with sufficient certainty. For example, the depth of a beam will affect its bending capacity and it will form part of d_c , while the beam span will affect the bending moment demand and will form part of d_d . On the other hand, the bending strength will form part of x_c while the actual applied load will be included in x_d . In practical problems the random vectors x_c and x_d may include many random variables. Very often, neither the function C nor D can be given explicit form, and they are only known as discrete results from numerical calculations using the computational models. In this case, it is convenient to give C or D a mathematical representation by fitting the numerical results with one of different types of *response surfaces* (Bucher et al.,1990; Faravelli,1989).

When the performance function is written as shown in Eqn.(1), non-performance will correspond to situations where the variables combine to make $D > C$, or $G < 0$. Thus, estimating the probability of non-performance is equivalent to estimating the probability of the event $G < 0$. This will be the *"probability of failure"* P_f , and the *reliability* will then be the complement $1.0 - P_f$.

The calculation of reliability requires statistical information for the different random variables. For example, the bending strength capacity of a composite will depend on the strength of the fibers, the properties of the matrix and the fiber volume percentage in the mix. Statistics for each of these components has to be determined from appropriate tests. Some variables may have more influence than others and, accordingly, they will require a more precise statistical description. Some demand variables will rely on available data, for example, wind speeds, river flows, depth of snow packs, quantity of rain, historical earthquake intensities, or occupancy loadings. Of course, there may be some variables for which no data or very little information are available. In this case, subjective estimates of the variability may be introduced in order to study the importance of such assumptions in the overall reliability of the system. Should a particular variable be found to be quite important but lacking detailed information, more effort should be spent in obtaining more data to avoid a corresponding penalty in the reliability estimate.

Apart from obtaining the solution of a problem with a better representation of reality, the use of reliability or probabilistic concepts offers many advantages not adequately addressed by more traditional, deterministic calculations. The calculated reliability in a given limit state will decrease if the information is sketchy or if the variability is high. Conversely, a premium is received through better information on the material, better modeling, or better procedures for quality control. In this sense, probabilistic methods encourage innovation in applications and manufacturing.

How do we implement, in practice, reliability calculations? One simple approach is by sampling values of the intervening variables *x*, from their corresponding probability distributions, and verifying whether the function *G(x)* results positive or negative. If $G(x) < 0$, then the particular sample of variables leads to system failure. By maintaining a counter of the

number of failures, N_f, observed in a sequence of N sample sets, the probability of failure can be estimated as the ratio

$$P_f \cong \frac{N_f}{N} \tag{2}$$

This process is known as a *Monte Carlo* simulation. The result will be different if the process is repeated for another sample of N selections. The variability in the results depends on N, diminishing as N increases, and the estimate will converge to the exact probability as N becomes large. This convergence is an advantage of the simulation procedure. However, if the system being analyzed has a low probability of failure, for example, 10^{-6}, it would be necessary to perform, on average, $N = 10^6$ samplings to expect to find one case of non-performance. Since this is the number of times that the function $G(x)$ would have to be evaluated, the procedure could be quite time consuming, particularly when this evaluation requires the running of a separate computer program to calculate either the capacity or the demand (e.g., a finite element program or a nonlinear dynamic analysis).

In a standard Monte Carlo simulation, the vectors x are chosen at random from their entire domain. In order to improve the efficiency of the simulation, techniques have been developed which permit a probability estimation with a reduced number of repetitions. These techniques, under the names of *Importance Sampling* or *Reduced Variance*, rely on selecting vectors x only within regions of importance, within which the combinations more likely to produce failure are located. These procedures are very effective and more detailed descriptions can be found in the literature (Ditlevsen, 1996; Schüeller et al., 1989). Still, many time-consuming evaluations of $G(x)$ may be needed.

Ingenious, although approximate, algorithms have been developed as alternatives to the simulation approach. These take the name of First Order Reliability Method (*FORM*) or Second Order Reliability Method (*SORM*). In particular, FORM (Rackwitz, 1978; Ditlevsen, 1981; Der Kiureghian, 1986) has become a standard approach because of its efficiency, although sometimes there is a tendency to forget that it is an approximate method that should be verified, when in doubt, by using a simulation approach.

2.1 First and Second Order Reliability Methods (FORM and SORM)

Given the practical importance of these methods, it is worthwhile to briefly comment on the details of their development.

In the multi-dimensional space of the variables x, the surface $G(x) = 0$ represents the boundary between the non-performance domain, $G(x) < 0$, and "survival" $G(x) > 0$. $G(x) = 0$ is called the "*failure surface*". Let us assume, for the moment, that the variables x are all independent (un-correlated) and Standard Normally distributed. That is, each has a mean = 0 and a standard deviation = 1. The origin O of the coordinates x correspond then to their mean values. Suppose that we generate a second set of variables y by rotating the axes x about the origin. This rotation implies a matrix linear transformation that does not alter neither the Standard Normal character nor the independence of the variables. Suppose further that the rotation is done in such a way that one of the new axes, for example, y_1, becomes normal to the surface $G(x) = 0$ at a point P. The distance from O to P is then a minimum distance between the origin (or mean point) O and the failure surface, a distance that is noted with β (*the reliability index*). *If the failure surface were to be linear* (a hyper-plane), then the entire non-performance domain would be characterized by the simple equation $y_1 > \beta$ and, since y_1 is a Standard Normal, the corresponding probability of failure would be given by the Standard Normal function Φ evaluated at (-β):

$$P_f = \Phi(-\beta) \tag{3}$$

The method is then very straightforward. A requirement is to find the minimum distance β between a point (O) and the failure surface *G(x) = 0,* and the corresponding failure probability would then follow from the tabulated Normal function, using Eqn.(3). It should be emphasized that the approximation of the method stems from the condition that the variables be all Normal and uncorrelated, and that the failure surface can be approximated as a hyper-plane. The first two conditions can be met by transformations (Der Kiureghian, 1986), regardless of the actual probability distribution of the variables or their correlation structure. These transformations are implemented in all the available software. Nothing can be done about the nonlinearity of the failure surface, and there lies the main source of the approximation. The algorithm to obtain β could be any optimization algorithm for the minimum distance, but schemes based on Newton's rule for roots of polynomials have been developed and are commonly implemented in reliability software (Hasofer and Lind, 1974).

The procedure is represented in Figure 1, where the function *G(x)* is shown along the vertical axis and the components of the vector *x* occupy, schematically, the horizontal plane. The failure surface *G(x) = 0* is then the intersection of *G* with the horizontal plane, and the reliability index will be the length between point *O* and *P*, located at a minimum distance from *O* . Starting from an initial vector *x**, the algorithm replaces the real surface *G* with the tangent plane *Γ* at *x** . This plane intercepts *G(x) = 0* with a straight line, and the algorithm finds point *P** , at a minimum distance between that intercept and the origin *O*. Point *P** is then used as the new *x**, repeating the procedure until an eventual convergence to *P*. It can be shown that the coordinates of *P* correspond to sensitivity coefficients for β with respect to each of the variables *x*. Although this procedure, as all Newton schemes, is sensitive to using a good starting point, it usually converges rapidly. The number of evaluations of *G(x)* are limited to those required to obtain the value of the function $G(x^*)$ and its gradient at x^*, and this number is normally much smaller than that required by Monte Carlo simulation. The gradient can be calculated by finite differences, or can be explicitly obtained if the function *G(x)* = 0 has been given a mathematical form through the use of response surfaces.

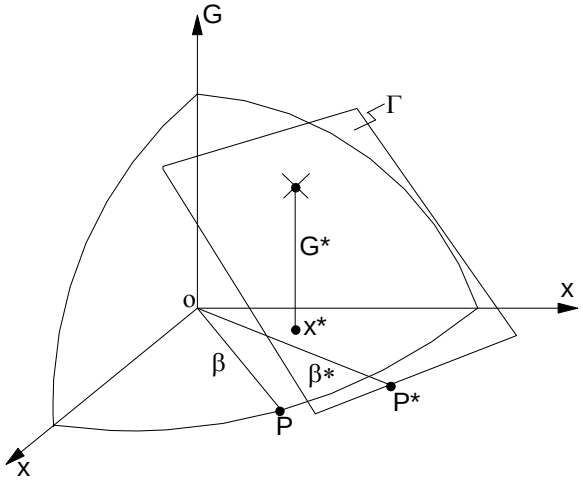

Figure 1. Iterative Algorithm to Find the Reliability Index β (Hasofer and Lind, 1974)

The accuracy of FORM depends then on the nonlinearity of the performance function *G(x)*. The prediction can be improved by using Importance Sampling simulation around the point *P*,

called the design point, the coordinates of which can be proven to be the most likely failure combination for the variables.

SORM is also based on finding the reliability index β, but instead of using Eqn.(3) to compute the corresponding probability under the assumption of a plane surface, it assumes that *G(x) = 0* is a parabolic surface sharing the same curvatures at P. This method sometimes gives better answers, but one can always construct examples for which, in fact, the linear approximation gives more accurate results.

Different software packages are now available to carry out calculations using FORM, SORM or different types of simulations. At the University of British Columbia we have developed our own, called RELAN (Foschi et al., 2000) and, more recently, Rt (Haukass et al., 2010). RELAN consists of a main body that executes all the algorithms, and a separate sub-program by means of which the user enters the specifics of the problem to be solved.

2.2 Response Surfaces

Many times the value of *G(x)* is the output of another computer program, for example, a dynamic analysis or a finite element calculation. In these cases, it may be inefficient to link directly the reliability index iteration with, for example, a finite element analysis. An alternative is to construct a *response surface* for the capacity or the demand, essentially evaluating *G(x)* ahead of time, at a sufficiently large number of combinations *x* (Faravelli, 1989; Liu and Moses, 1994). The discrete points thus obtained can be used to fit a mathematical representation for the response, and this representation is then used as a substitute for the actual *G(x)*. The fitted response $G_F(x)$ is then used for the reliability estimation to obtain a design point P and a reliability index β.

Different forms may be used for the fitted function $G_F(x)$. Bucher et al. (1997), for example, have considered polynomial expansions of the type

$$G_F(x) = a_0 + \sum_{i=1}^{N} a_i X_i + \sum_{i=1}^{N} b_i X_i^2 \qquad (4)$$

for N variables, and with 2N+1 coefficients found by regression of the discrete data. Other forms may be chosen to better represent the influence of a variable. For example, suppose that one of the variables is the load *Q* and that the response variable is the deflection of a laminated plate. Obviously, if there is no load *Q* there must not be any deflection. In this case, it is better to propose

$$G_F(x) = Q\Big[\ a_0 + \sum_{i=1}^{N} a_i X_i + \sum_{i=1}^{N} b_i X_i^2\ \Big] + Q^2\Big[\ c_0 + \sum_{i=1}^{N} c_i X_i + \sum_{i=1}^{N} d_i X_i^2\ \Big] \qquad (5)$$

A more complete discussion on applications of polynomial response surfaces in earthquake engineering is given by Möller (2003). General, flexible and useful response surfaces are given by *neural networks*, and several applications to earthquake engineering have been the subject of publications and of current research (Möller et al., 2009).

The approaches to reliability estimation have now been quite well studied, within the sound framework of probability theory. Integration of this knowledge with the advanced techniques of analysis in computational mechanics conforms to the ultimate objective of being able to not only analyze a complex problem but of also considering the reality and implications of uncertainty.

2.3 Simplifications for common use (Codes)

Carrying out a full reliability analysis is perhaps too large a task in many common situations, as it is to carry out a full finite element analysis. With this in mind, design guidelines or Codes implement simplifications that would result in designs that, if verified with a full probabilistic analysis, would be shown to have a minimum required reliability in most practical situations to which the Code is intended to apply.

The Code design equations generally contain formulas specifying characteristic values for the capacity and the demand, plus a sufficient number of "*factors*" to be applied to those characteristic values. These factors would have been chosen or calibrated in a manner such that, when using the Code, the resulting design would have achieved the minimum desired target reliability. Of course, with just a few factors, this target reliability cannot be satisfied uniformly for a large number of situations. As a result, the factors are calibrated by optimization, minimizing the difference between the target reliabilities and those achieved over a large number of design conditions to which the code would apply.

Although the Code approach simplifies the reliability consideration in practice, it has the disadvantage that the reliability achieved cannot be guaranteed to be as desired across situations not covered in the optimization. Furthermore, Code prescriptions for design of structures will lead to somewhat different reliability levels according to the geographical location, in accordance to changes in the snow or wind or earthquake demand statistics. The importance of the problem at hand would guide on whether applying simplified Code guidelines or implementing a comprehensive reliability evaluation.

2.4 The inverse problem of performance-based design

In practice, a very important problem is that of finding appropriate values for components of the vectors d_c or d_d (*design parameters*) so that the achieved reliabilities in different performance criteria satisfy minimum requirements and, in addition, the design satisfies a minimum requirement (minimum weight or total cost).

This is an optimization problem for the objective weight or cost, subject to minimum reliability constraints. It is currently generally known as *Performance-Based Design*. For example, what should be the dimensions of the columns in a building subject to uncertain earthquake ground motion, so that reliability indices achieved exceed minimum targets regarding maximum deformations and damage, while maintaining the total cost (construction plus repairs after an earthquake) at a minimum? This is a very interesting problem and the subject of continuing and current research (see, for example, Möller et al., 2009).

3 CASE STUDY 1: ICEBERG IMPACT WITH AN OFFSHORE STRUCTURE

It is useful to go through the steps of a practical application. The problem refers to the collision of an ice mass (an iceberg) with an offshore oil exploration/extraction platform. The problem uses data for one such platform (Hibernia), currently in use off the coast of Newfoundland (Canada). This platform is a gravity-based reinforced concrete structure, protected from iceberg impact by a concrete cylindrical wall. In this study, the structure is assumed to be a vertical circular cylinder with an external radius a = 58 m and located in a sea depth d = 80 m.

Of concern is the possibility of an iceberg colliding with the platform. Icebergs of different size float down from the Arctic, particularly in the spring and early summer, and the platform structure and its foundation have to be designed for a collision force that would have a specified low probability of being exceeded on an annual basis (for which the current

Canadian code CAN/CSA-S471(1992), specifies $1.0x10^{-4}$). A more complicated problem adds the influence of high seas and waves in combination with an iceberg (Foschi et al., 1998).

The model for the maximum iceberg load on a structure is obtained by an energy balance in which the initial kinetic energy of the iceberg is equated to the energy dissipated through ice crushing up to the time the iceberg is brought to rest. Although it could be taken into account, the energy dissipation through structural damage or ductility is not included here. The limit state or performance function *G* of interest relates to the exceedence probability of a load level F_o,

$$G(x) = Fo - F_M(x)R_{n1} \tag{6}$$

where $F_M(\mathbf{x})$ is the maximum force developed on the structure, **x** denotes a set of specified random variables characterizing the structure, the iceberg conditions, and R_{n1} is a random variable associated with model inaccuracy in the calculation of F_M .

The probabilities of failure p_e are obtained by FORM on the condition that the impact has occurred. The *annual exceedence probabilities*, denoted as p_a, are obtained by using the hypothesis that the events (i.e. iceberg collision arrivals) follow a Poisson pulse process with a given mean rate of annual occurrence (events per year), denoted μ. Thus,

$$p_a = 1 - \exp(-\mu p_e) \tag{7}$$

3.1 Iceberg shape and size

Of course it is very difficult to represent accurately the three-dimensional shape of a realistic iceberg by a mathematical equation. The approach adopted here follows that of Det Norske Veritas (1988), in which the iceberg is assumed to be circular in plan and ellipsoidal in elevation Fig. 2, with horizontal (major) and vertical (minor) semi-axes R and B respectively. From statistical data for the Grand Banks off Newfoundland, all the iceberg dimensions are expressed in terms of a single random variable L (in m) which is represented by a Gamma distribution, with a mean value 121.60 m and a standard deviation 56.70 m. Other characteristic dimensions of the iceberg may be expressed in terms of L. In particular, the horizontal semi-axis R, and the iceberg diameter at the waterline D are given respectively as:

$$R = 0.428L + 1.053L^{0.63} \tag{8}$$

$$D = 0.679L + 1.671\,L^{0.63} \tag{9}$$

It can be shown that the vertical semi-axis B, and the iceberg height above the water, b, are related to the draft h according to, respectively:

$$B = \frac{h}{1.608} \tag{10}$$

and

$$b = 0.244\,h \tag{11}$$

The iceberg draft h is in turn related to L, except that icebergs capable of colliding must have a draft smaller than the water depth d = 80 m. Thus:

$$h = \text{Min}\begin{cases} 3.781L^{0.63} \\ d \end{cases} \tag{12}$$

Using the specified Gamma distribution for L, Eqn.(12) is used to obtain a corresponding distribution of the draft h. Taking account of the truncation at a maximum of 80 m, the data

for h have been fitted with a Beta distribution with a minimum of 0 m and a maximum of 80 m, resulting in a mean draft 61.35 m with a standard deviation 12.38 m.

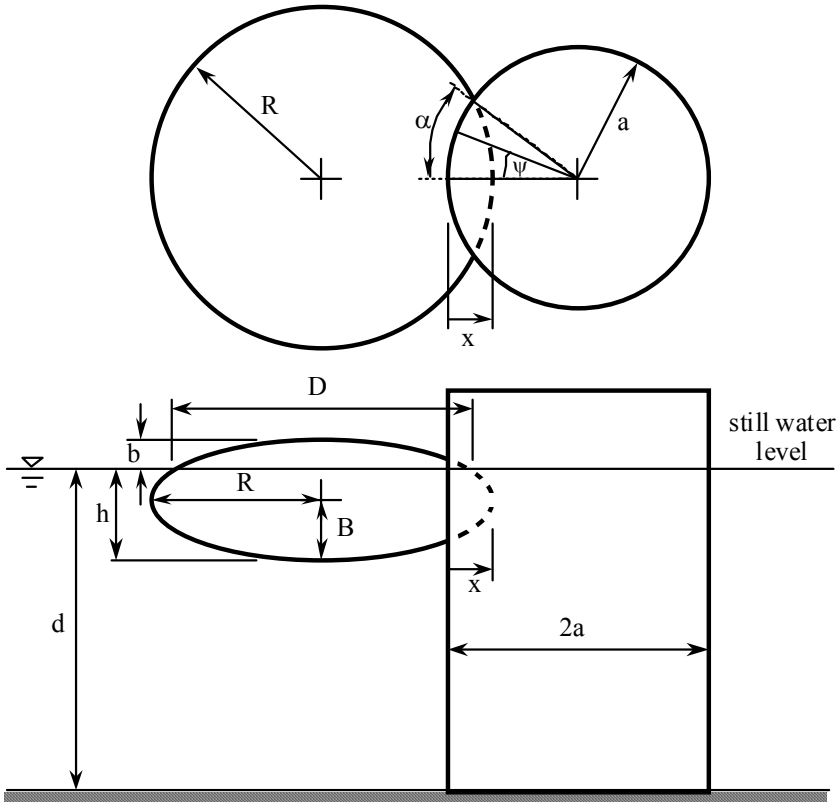

Figure 2. Iceberg-structure geometry

3.2 Ice crushing pressure

The force developed during an iceberg collision varies during the process of ice crushing against the structure, since the area of contact is continuously changing and the crushing pressure exhibits a notable size effect (the greater the contact area, the lower the required crushing pressure). For different penetrations *x* into the ice, as shown in Fig. 2, it is possible to compute the area of contact as the intersection of the ellipsoid with the cylindrical structure of radius a. From a knowledge of the relationship between ice-crushing pressure and area, the force *F(x)* may then be obtained by integration, assuming that the pressure is uniformly distributed over the area. The impact is assumed to be head-on, and the contact area is computed accordingly. The pressure p required to crush the ice depends on the area of contact A. It is assumed that the crushing pressure p has a lognormal distribution, with mean m_p and coefficient of variation V_p. Therefore:

$$p = \frac{m_p}{\sqrt{1+V_p^2}} \exp\left[R_{n4}\sqrt{\ln(1+V_p^2)}\right] \tag{13}$$

where R_{n4} has a Standard Normal distribution (mean of 0, and a standard deviation of 1).

In general, the size effect for the mean pressure m_p can be written in the form:

$$m_p = \text{Max.}\begin{cases} C_1 A^{C2} \\ p_o \end{cases} \tag{14}$$

Although data on iceberg (old) ice are scarce, the scatter in the available information for ice in Arctic conditions is reasonably well represented with the following parameters :

$$\begin{aligned} V_p &= 0.50 \\ C_1 &= 9.0 \text{ MPa} \\ C_2 &= -0.5 \\ p_o &= 2.0 \text{ MPa} \end{aligned} \tag{15}$$

with A in m^2. The value p_o is a lower bound for m_p. Due to uncertainty in ice crushing pressure for large areas A, it may be more appropriate to represent p_o by a suitable probability distribution. Instead, in the present discussion, p_o is taken as a constant. It should be noted that the lower bound p_o= 2 MPa is reached at a contact area of about 20 m^2, which is probably very quickly exceeded during a collision. The value of p_o is not well defined from available data, and since it is expected to have marked influence on the loads developed during the collision, three specific values of p_o are studied: 2, 4 and 6 MPa.

3.3 Force-penetration relationship

For a given penetration *x* due to ice crushing (see Fig. 2), the force *F(x)* acting on the structure can be calculated from an integration of the crushing pressure p over the area of contact A(x):

$$A(x)=2a\int_0^{\alpha} s(x,\psi)\, d\psi \tag{16}$$

and then

$$F(x) = 2a\int_0^{\alpha} p(x)\ \ s(x,\psi)\cos\psi\, d\psi \tag{17}$$

where the angles α and ψ are shown in Fig. 2, and s is the height of the contact area corresponding to the angle ψ.

3.4 Impact velocity

An iceberg will impact the structure with a velocity V which influences the magnitude of the maximum iceberg force on the structure. The impact velocity V is generally determined by the prevailing current, wind, and waves. For simplicity, the impact velocity V in calm water (iceberg alone, no wind or waves) is taken here to be equal to the ocean current velocity U:

$$V = U \tag{18}$$

Following data from Det Norske Veritas (1988), the current U at the location of the platform is assumed to possess a lognormal distribution, with a mean of 0.32 m/sec and a standard deviation 0.27 m/sec.

For a relatively small iceberg with R < a, and assuming sufficient kinetic energy, the iceberg could eventually disintegrate against the structure; for a large iceberg with R > a, the

structure would split the iceberg in two. However, these two situations represent extreme events. For the general case, the iceberg will be stopped after a few meters of penetration.

3.5 Maximum force

In calm water, the calculation model for the maximum force F_M is implemented through consideration of an energy balance. The iceberg will be stopped when its kinetic energy is fully dissipated through ice crushing up to a penetration x_C,. Thus, this energy balance may be expressed as:

$$\frac{1}{2} M (1 + C_m) V^2 = \int_0^{xc} F(x)\, dx \tag{19}$$

where the iceberg mass M has been augmented by the added-mass coefficient C_m accounting for hydrodynamic effects. The right-hand side corresponds to the energy dissipated through ice crushing up to the penetration x_C, which is then obtained by iterations using Eqn.(17) and Eqn.(19) for a given iceberg geometry, impact velocity and crushing pressure parameters.

Once x_C is found, the maximum force F_M to be entered in the performance function of Eqn.(6) is obtained from the force-penetration relationship F(x).

3.6 Added Mass

The added-mass of an iceberg at impact, C_m, depends on its submerged geometry, the water depth and the submerged geometry of any neighboring structure (and thus it is a function of the iceberg distance from any such structure). It is determined by solving the boundary value problem corresponding to an iceberg undergoing small amplitude oscillations in otherwise still water. A description of the calculation procedure has been given by Isaacson and Cheung (1988a, b). In general, the added-mass is frequency- dependent, although it is customary to use a single value (usually the zero frequency value) when treating the iceberg impact problem. The zero-frequency added-mass was estimated here for a range of iceberg parameters, both in open water and when in contact with the structure. A simple expression (a response surface) has been derived from numerical results obtained over a range of conditions:

$$C_m = 0.0883 \left(\frac{D}{d}\right)\left(\frac{h}{d}\right) + 0.6386 \left(\frac{h}{d}\right) - 0.0998 \left(\frac{D}{d}\right) + 0.2229 \tag{20}$$

3.7 Comparison between FORM results and Monte Carlo simulations

It is useful to compare the accuracy of the FORM results against those of Monte Carlo simulations (10^6 samples). Figure 3 shows the exceedence probabilities associated with different load levels F_o. For this comparison, p_O = 2 MPa and V_p = 0.5. The model error variable R_{n1} is assumed normally distributed, with a mean of 1 and a standard deviation of 0.15. At 500 MN, the design point P includes a current velocity V = 0.55 m/sec and an iceberg of dimensions L = 143.0 m and h = 67.9 m. From higher to lower, the sensitivity of the results to variable uncertainty is ordered as follows: V, L, h, ice crushing variable R_{n4}, and model uncertainty R_{n1}. It is apparent from Fig. 3 that FORM produces excellent results in comparison to simulation, even for this nonlinear problem. FORM also results in very efficient and fast calculations.

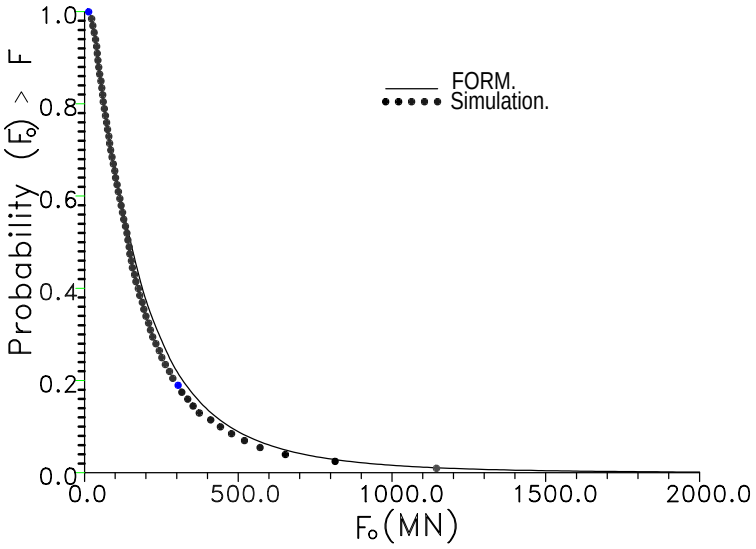

Figure 3. Comparison between FORM and Monte Carlo simulations for exceedence probability of different iceberg impact force levels F_o

3.8 Results

Table 1 shows a summary of the statistical parameters that have been used for the various specified random variables, except that the parameters for the iceberg draft h are determined by those of L according to Eqn.(12).

Variable	Distribution	Characteristics
Iceberg length, L	Gamma	Mean = 121.60 m Std.Dev. = 56.70 m
Iceberg draft, h	Beta	Mean = 61.35 m Std.Dev. = 12.38 m Min. = 0.00 m Max. = 80.00 m
Current velocity, U	Lognormal	Mean = 0.32 m/sec Std.Dev = 0.27 m/sec
R_{n1}, model uncertainty	Normal	Mean = 1.0 Std.Dev.= (input)
R_{n4}, ice crushing pressure p	Normal	Mean = 0.0 Std.Dev.= 1.0

Table 1. Summary of random variables and their statistics.

A program ICELOAD was run to obtain the forces for iceberg collision at annual exceedence probabilities of $1x10^{-2}$ and $1x10^{-4}$ (respectively, 100 and 10000-year events) and the corresponding results are shown in Table 2. ICELOAD was a name given to the RELAN adaptation for the specific performance function of this problem.

. Table 2 indicates the influence on the annual exceedence probability of the iceberg collision arrival rate μ, and the ice crushing pressure lower threshold p_o. The table indicates that the iceberg collision forces are strongly dependent on these factors.

Annual exceedence probability	Iceberg arrival rate μ (events/year)	Maximum iceberg collision force F_M (MN)		
		p_o = 2 MPa	p_o = 4 MPa	p_o = 6 MPa
10^{-2}	0.04	248	351	431
	0.08	381	537	657
	0.20	587	830	1,017
	1.00	1,061	1,503	1,843
10^{-4}	0.04	1,605	2,276	2,792
	0.08	1,932	2,740	3,360
	0.20	2,425	3,442	4,224
	1.00	3,484	4,952	6,080

Table 2. Maximum iceberg force F_M for annual exceedence probabilities of 10^{-2} and 10^{-4} , for various iceberg collision arrival rates μ and ice crushing pressure threshold p_o.

4 CASE STUDY 2: VESSEL IMPACT WITH A BRIDGE PIER

This second example also concerns a collision study and the use of probabilistic concepts. Several new bridges have been built in British Columbia across the Fraser River, a major navigational route for vessels carrying containers, mining and forest products. The Fraser starts in the Rocky Mountains and reaches the Pacific at the city of Vancouver. The bridges were built in connection with infrastructure funding for the 2010 Winter Olympics. Figure 4 shows the Golden Ears bridge, a cable stayed structure with several spans.

Figure 4. Golden Ears Bridge across the Fraser River, British Columbia

Given the river traffic there exists the possibility of a collision between the vessels and any of the bridge piers. The collision force F depends on several random variables: the vessel traffic density (number of trips per year), the vessel size (tonnage), the vessel speed with respect to the water, the river current, the vessel position within the navigation channel when in distress, the river flow at different times of the year, and the effect of the tides (all bridges are located at a relatively short distance from the sea).

According to requirements of the Canadian Highway Bridge Code CAN/CSA-S6(2010), the force F must be calculated in correspondence with a $1x10^{-4}$ annual exceedence probability. The Code also specifies a simplified calculation model for the force in terms of the kinetic energy of the vessel and the energy dissipation capacity of the pier. Thus, assuming an elastic structure with stiffness K, and being M and V, respectively, the mass and the speed of the vessel, the balance of energy at the end of the collision penetration x requires

$$MV^2 / 2 = K x^2 / 2 \qquad (21)$$

from which the maximum penetration x is

$$x = (M/K)^{1/2} V \qquad (22)$$

The maximum force developed during the collision is then shown to be of the form

$$F = \lambda M^{1/2} V \qquad (23)$$

with λ being a constant that reflects the system of units and the stiffness of the system. The Canadian Code gives the equation

$$F = M^{1/2} V / 8.4 \qquad (24)$$

for which the mass of the loaded vessel M must be given in Tonnes and corresponds to the "Dead Weight Tonnage", not including the mass of the empty vessel; V is the collision speed (resultant of the vessel speed with respect to water, the river current and the tides) in m/sec. Eqn.(24) is calibrated to give the force F in MN. The performance function G for the problem is as in Eq.[6], and the reliability analysis is applied to obtain the probability that the collision force F exceeds different thresholds F_o

$$G = F_o - F R_n \qquad (25)$$

As in Eqn.(6), R_n is a random variable accounting for the uncertainty in the calculation model for the force.

For each threshold F_o , Eqn.(25) allows the estimation of the exceedence probability when a collision has taken place. The annual risk of exceeding F_o must be calculated with Eqn.(7), using the annual mean arrival rate of the collisions, μ . This is estimated from

$$\mu = N P_G P_A P_\theta \tag{26}$$

In Eqn.(26), N is the traffic density (number of trips per year for a particular vessel type); P_G is the geometric probability that a vessel, navigating out of control, will come into contact with the bridge pier; P_A is the probability that a vessel will be in distress or out of control; and P_θ is a factor which incorporates the effect of the river geometry in the vicinity of the bridge (straight approach vs. bends).

N is obtained from traffic data, and should include estimates of future traffic. These data are usually provided by river or port authorities. The geometric probability P_G assumes that the navigation position of a vessel in distress, with respect to the center of the navigation channel, is a Normal random variable, with a mean of 0 and a standard deviation equal to the length of the vessel. This assumption is incorporated in the Code on the basis of data from previous collisions in different countries. The probability P_A includes the "aberrancy" probability that a vessel is out of control, and is obtained from data on historical vessel navigational incidents: The Code uses the value 1.2×10^{-4} for barges pulled by tugboats. In addition, P_A contains a factor for the type of traffic, related to the possibility of vessels crossing or overtaking each other at the bridge location. The value used for this factor is 1.3, corresponding to an average traffic density, when vessels occasionally meet, pass or overtake each other in the immediate vicinity of the bridge.

The calculation of the total annual risk of exceeding a threshold F_o is done by adding the annual risk contributions from all the collision scenarios or vessels (considering their individual characteristics and whether they are travelling up or downstream, with or against the tide direction). The final result for the force F would then correspond to a total annual risk, specified by the Code, of 1.0×10^{-4}.

The velocity V is obtained from hydraulic information. Data for the Fraser river show a maximum flow discharge during the month of June, and minima during the winter season (December, January, February and March). Intermediate flows are recorded during the in-between months. River flow statistics are first obtained for each season and, assuming that the collision could occur at any time of the year, the river discharge at the time of the collision has a distribution which is obtained from the seasonal discharges weighted according to their respective yearly durations. The weighted distribution for the flow *Q* was represented as an Extreme Type I with a mean of 4280 m^3 /sec, and a standard deviation of 2607 m^3/sec.

Figure 5 shows the measured velocity V at different flows Q, the latter corresponding to the station Mission, close to and upstream from the bridge location. The minimum and maximum velocities include the effect of the tides, which are seen to become very important during the low flow months of winter. Figure 5 shows, in fact, that at high tide the resultant current velocity is at its minimum and becomes negative during low river discharges. The data from Figure 5 are used to represent the relationship between mean current speed, V_C , and the standard deviation σ_V , at a particular value of Q:

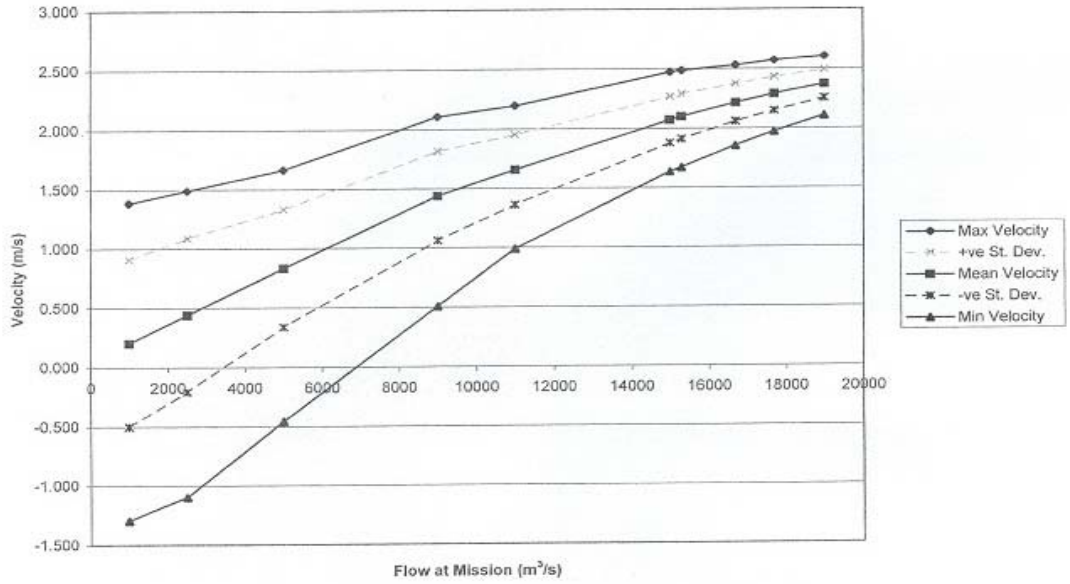

Figure 5 River Current Velocity (m/sec) vs. River Discharge Flow (m^3/sec)

$$\text{Mean } \overline{V}_C = 0.223 + 0.199x10^{-3}Q \text{ (m/sec.)} \tag{27}$$

$$\text{Standard Deviation } \sigma_{V_C} = 0.698 \exp(-0.232 \times 10^{-3}Q) \text{ (m/sec.)} \tag{28}$$

Finally, using Eqns.(27) and (28), the current speed V_C at collision can be assumed to have a Normal distribution conditional on the value of Q :

$$V_C = \overline{V}_C(Q) + R_{N1}\sigma_{V_C}(Q) \tag{29}$$

in which R_{N1} is a Standard Normal random variable . Since the collision could take place at any time of the tidal cycle, an alternative to Eqn.(29) would be a Uniform distribution for V_C between its minimum and maximum values from Figure 5.

The vessel traverses with a speed V_W with respect to the water. The final collision speed is then $V = V_W + V_C$ or $V = V_W - V_C$, depending on whether the vessel is travelling downstream or upstream. V_W is also considered a random variable, Normally distributed, with a mean of 3.5 m/sec. and a standard deviation of 0.25 m/sec. To maintain steerage and control of the tugboat, however, V_W has a minimum of 3.0 m/sec (from pilot's data).

4.1 Results

As shown in Figure 4, the bridge has four piers, from South to North (right to left in the Figure): S1, S2, N2 and N1. The following Table 3 shows the corresponding final collision loads at an annual exceedence probability of $1.0x10^{-4}$, considering a total of 32 vessel scenarios. The loads shown in Table 3 are used for the design of the piers' pile foundations. A final, more refined analysis can then be carried out taking into account the energy dissipation through foundation non-rigidity, using models for soil-structure interaction.

The reliability analysis allows the identification of the "controlling" vessel, that which has the largest contribution to the total annual risk. Likewise, the analysis allows the identification of the most important variables in the problem and, for example, the formulation of policies for navigational restrictions: should traffic be allowed with outgoing tides during the high river flow periods? Finally, since the results could be altered by changing the bridge configuration (distance between piers) in relation to the width and location of the navigation channel, the reliability study could form part of the total cost optimization for the bridge. All of these are important design considerations which are facilitated by the probabilistic approach to the problem.

Pier	Collision Force (MN) (Exceedence Probability $1.0x10^{-4}$)
N1. N2	74.9
S1, S2	59.0

Table 3. Results Pier Collision Loads, Piers N1, N2, S2 and S1

CONCLUSIONS

Theoretical models for computational mechanics should include information on the uncertainties of the intervening variables, so that probabilistic statements can be given for the outputs. This is becoming more and more important as engineering analyses must address questions of risk in a quantitative manner. There is no other approach to answer, with sufficient confidence, questions about the risks to infrastructure from hazards like earthquakes, floods or high winds, or similar environmental engineering questions like seepage of pollutants or hazards to water quality. Quantitative assessment of risks is essential to allocation of funds for construction and maintenance of different systems.

In order to achieve these objectives, the advances in computational mechanics must be complemented with the advances in applications of probability theory to engineering problems. In the future, common use of these techniques may replace the approximate, more simplistic approaches in current design procedures or Codes of practice. In fact, many current applications are not entirely governed by Codes and require a full reliability treatment. Two examples of such an application have been shown here, to answer the question of what level of force should be used to design an offshore platform or a bridge pier, at a given level of risk, when the hazard is either the collision with an iceberg or with a passing vessel.

A common objection to the application of probabilistic methods is the possible lack of data (even when uncertainties are acknowledged). It should be apparent that the same lack of data is nevertheless present even when using deterministic approaches, producing a false sense of confidence in the results. The answer to lack of information should be to use judgement and assume some range of values for those variables lacking data, carrying out the probabilistic analysis and seeing (from FORM, for example) whether those variables are indeed important to the results. Should they be, then there is no choice other than collecting more information.

Linking computational mechanics procedures with probabilistic approaches offers not only a more realistic solution to problems, but many new avenues for theoretical and applied research.

REFERENCES

Bucher, C.G. and Bourgund, U. , A Fast and Efficient Response Surface Approach for Structural Reliability Problems. *Structural Safety*, 7: 57-66, 1990.

CAN/CSA-S6, Canadian Highway Bridge Design Code, Canadian Standards Association, Ottawa, Ontario, 2010.

CAN/CSA-S471, Canadian Code for Offshore Structures, Canadian Standards Association, Ottawa, Ontario, 1992.

Der Kiureghian, A.and Liu,P.,Structural Reliability Under Incomplete Probability Information. *Journal of Engineering Mechanics*, *ASCE*. 112:1,1986.

Det Norske Veritas, Probabilistic framework for ice loads on fixed marine structures. Calgary. Report to Department of Public Works, Ottawa, Vol. 1, 1988.

Ditlevsen, O., Principle of Normal Tail Approximation. *Journal of Engineering Mechanics, ASCE*. 107:6,1191-1208, 1981.

Faravelli, L., Response Surface Approach for Reliability Analysis. *Journal of Engineering Mechanics, ASCE*. 115: 2763-2781, 1989.

Foschi, R.O., Li, H., Folz, B., Yao, F. and Baldwin, J. RELAN: A General Software Package for Reliability Analysis. Department of Civil Engineering, University of British Columbia, Vancouver, Canada, 2000.

Foschi, R.O., Isaacson, M., Allyn, N. and Saudy, I. Assessment of the Wave-Iceberg Load Combination Factor, *International Journal of Offshore and Polar Engineering*, 8: 1-8. 1998.

Hasofer, A.M. and Lind, N.C., Exact and Invariant Second-Moment Code Format. *Journal of Engineering Mechanics, ASCE*. 100:1, 111-121,1974.

Isaacson, M., and Cheung, K.F. , Hydrodynamics of an ice mass near an offshore structure. *Journal of Waterway, Ports, Coastal and Ocean Engineering*, 114:4, 487-502, 1988*a*.

Isaacson, M., and Cheung, K.F., Influence of added mass on ice mass impacts. *Canadian Journal of Civil Engineering*, 15:4, 698-708, 1988*b*.

Möller, O. and Foschi, R.O. Performance-Based Design: A Response Surface Methodology, *Earthquake Spectra*, 19:3, 579-603, 2003.

Möller, O., Foschi, R.O., Quiroz, L. and Rubinstein, M. Structural Optimization for Performance-Based Design in Earthquake Engineering: Applications of Neural Networks, *Structural Safety* 31: 490-499, 2009.

Rackwitz, R. and Fiessler, B. Structural Reliability under Combined Random Load Sequence. *Computers and Structures*, 9:5,489-494, 1978.

Schüeller, G.I., Bucher, C.G. and Bourgund, U., On Efficient Computational Schemes to Calculate Structural Failure Probabilities. *Probabilistic Engineering Mechanics*, 4:1, 10-18, 1989.

The subject of reliability theory in engineering applications is the topic of several excellent books:

Ang, A.H. and Tang, W., *Probability Concepts in Engineering Planning and Design*, Volume II-Decision, Risk and Reliability, John Wiley and Sons, 1984.

Ditlevsen, O. and Madsen, H.O. , *Structural Reliability Methods*. John Wiley and Sons, 1996.

Hurtado, J.E., *Structural Reliability, Statistical Learning Perspectives*, Springer Verlag, 2004.

Madsen, H.O., Krenk, S. and Lind, N.C. , *Methods of Structural Safety*. Prentice-Hall,1986.

Melchers,R., *Structural Reliability: Analysis and Prediction.* Ellis Horwood Limited,UK,1987.

Myers, R. and Montgomery, D., *Response Surface Methodology*, John Wiley and Sons, 1995.

Thoft-Christensen, P. and Baker, M. Structural Reliability Theory and Its Applications. Springer-Verlag. 1982.
Thoft-Christensen, P. and Murotsu, Y. Application of Structural Systems Reliability Theory. Springer-Verlag. 1986.
Wen, Y.K. 1990. Structural Load Modeling and Combination for Performance and Safety Evaluation. Elsevier.